외계행성 대기
Exoplanetary Atmospheres

Lecture 1: Introduction and Observational Techniques
2026 September 7 (Monday)

Based on: Chapter 1 of Seager, *Exoplanet Atmospheres* (2010) and Chapter 1 of Heng, *Exoplanetary Atmospheres: Theoretical Concepts and Foundations* (2017)

선광일 (Kwangil Seon)
KASI / UST

2026-09-07 00:33

Outline – Lecture 1

Why Study Exoplanet Atmospheres?

The Birth of Exoplanetary Science

Two Paths to Observing Exoplanet Atmospheres

Transits and Occultations in Detail

Radial Velocities, Direct Imaging, and Microlensing

Types of Planets

Outlook and Summary

The big questions

The search for our place in the cosmos is thousands of years old. For the first time we have the technology to attack questions such as

"Do other Earths exist?" *"Are they common?"* *"Do they harbor life?"*

Critical to deciding whether a planet is **habitable** or **inhabited** is an understanding of its **atmosphere**:

- Almost all information about the *temperature* and the *chemical abundances* of a planet comes from atmospheric **photometry** or **spectroscopy**.
- The atmosphere is the only part of a distant planet that we can probe remotely; the interior and the surface are inferred indirectly (bulk density, spectral features).
- The same physics — radiative transfer, chemistry, dynamics — applies to all planets, so exoplanet atmospheres are also a laboratory for understanding the Solar System in a wider context.

This course develops the *theoretical* tools needed to interpret such observations. Today: what is observed, how, and for what kinds of planets.

Earth as an exoplanet: the pale blue dot

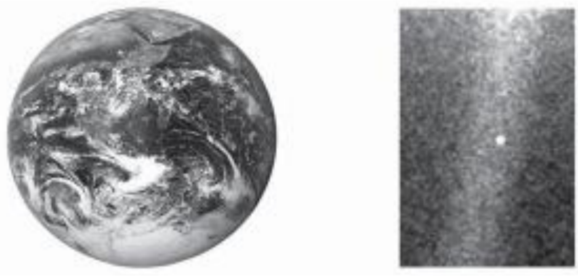

Figure 1: Earth from space. Left: Apollo 17 (1972). Right: Voyager I from more than four billion miles; Earth sits inside a band of light scattered in the camera optics. Reproduced from Seager (2010), Fig. 1.1.

Ultimately we would like an image of an Earth twin as beautiful as the Apollo image. For our generation, exoplanets are instead **spatially unresolved** — point sources.

Voyager I saw Earth this way: all surface and atmospheric features are hidden inside a single speck of light.

What survives in a point source?

- total brightness (photometry),
- brightness temperature,
- the **spectrum** (hemispherically averaged),
- time variability (rotation, orbital phase).

Everything we learn about an exoplanet atmosphere must be extracted from these.

What a disk-averaged spectrum contains (1): reflected light

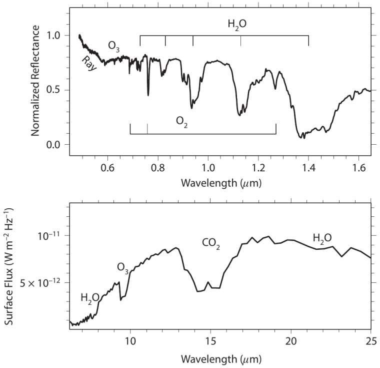

Figure 2: Earth's hemispherically averaged spectrum: visible (Earthshine, Turnbull et al. 2006) and mid-infrared (Mars Global Surveyor, Pearl & Christensen 1997). Seager (2010), Fig. 1.2.

Earth itself has been observed "as an exoplanet." In the **visible and near-infrared** the light is reflected sunlight, and the spectrum is shaped by scattering and absorption in the atmosphere:

- The reflectance rises toward the blue: *Rayleigh scattering* by N_2 and O_2 molecules — the reason the sky is blue and the pale dot is blue.
- O_3 absorbs in the broad Chappuis band ($\sim$0.5–0.7 μm).
- The narrow O_2 A band at 0.76 μm (and the B band at 0.69 μm).
- H_2O bands at 0.72, 0.82, 0.94, 1.13, and 1.4 μm grow progressively deeper toward the near-infrared.

The strengths of these bands depend on the column of absorber *above* the reflecting surface or cloud, and on the cloud cover itself, so a disk average mixes clear and cloudy scenes.

What a disk-averaged spectrum contains (2): thermal emission

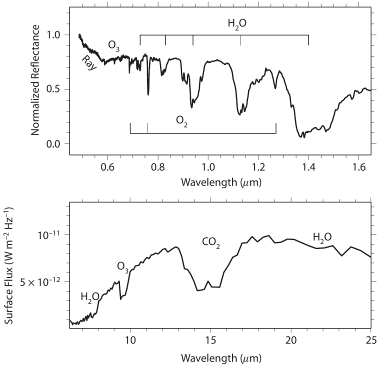

Figure 3: Same as the previous slide; the bottom panel is thermal emission from the surface and atmosphere. Seager (2010), Fig. 1.2.

In the **mid-infrared** the planet shines by its own *thermal emission*, roughly a ∼290 K Planck curve from the surface, cut by absorption bands of the cooler atmosphere above it:

- The 15 μm CO_2 band and the 9.6 μm O_3 band are the deepest features.
- H_2O absorbs at $\lambda < 8\,\mu m$ and $\lambda > 18\,\mu m$; the 8–12 μm "window" shows the warm surface.
- Band *depths* probe the vertical temperature structure (the band core forms high, where it is cold); the continuum probes the surface or cloud-top temperature.

Lesson: a spectrum encodes both the *composition* and the *temperature* of an atmosphere. The simultaneous presence of O_2, O_3, and H_2O is a potential *biosignature*. Later chapters develop the radiative-transfer tools to model such spectra quantitatively.

The real obstacle: planet-star contrast, not faintness

We cannot yet detect and study an Earth twin. The reason is *not* intrinsic faintness — exoplanets are no fainter than the faintest galaxies observed by the Hubble Space Telescope. The problem is that the planet sits right next to a star that is enormously brighter, only a fraction of an arcsecond away.

Visible-wavelength contrast F_p/F_*	Earth–Sun twin	Jupiter–Sun twin
(Seager 2010)	2.1×10^{-10}	1.4×10^{-9}

- To see an Earth twin in visible light one must isolate a signal ten billion times fainter than the star. Even a Jupiter twin is only about one part in a billion.
- Scattered starlight in the telescope optics (diffraction, speckles from wavefront errors) swamps the planet at these contrast levels; hence coronagraphs, adaptive optics, and starshades.
- The contrast, not the photon count, sets the difficulty. This motivates looking for situations where the contrast is *intrinsically* more favorable.

Where do the contrast numbers come from?

A planet's light has two contributions.

- **Reflected starlight.** The planet intercepts a fraction $\pi R_p^2/(4\pi a^2)$ of the stellar luminosity and reflects part of it back toward the observer. At full phase

$$\left.\frac{F_p}{F_*}\right|_{\rm refl} = A_g \left(\frac{R_p}{a}\right)^2, \qquad \left(\frac{R_\oplus}{1\,\mathrm{AU}}\right)^2 = 1.8\times 10^{-9},$$

  where A_g is the *geometric albedo* (Earth $\sim$0.2–0.4). Averaging over orbital phase (only part of the illuminated hemisphere is visible) brings an Earth twin to the 10^{-10} level.

- **Thermal emission.** Treating star and planet as blackbodies,

$$\left.\frac{F_p}{F_*}\right|_{\rm therm} = \left(\frac{R_p}{R_*}\right)^2 \frac{B_\lambda(T_p)}{B_\lambda(T_*)}.$$

  The Planck ratio grows rapidly toward the infrared: in the Rayleigh–Jeans limit it tends to $(R_p/R_*)^2\, T_p/T_*$, which is far larger than the exponentially suppressed ratio on the Wien side. Thermal emission is therefore the way to beat the contrast problem, provided the planet is warm.

Contrast versus wavelength

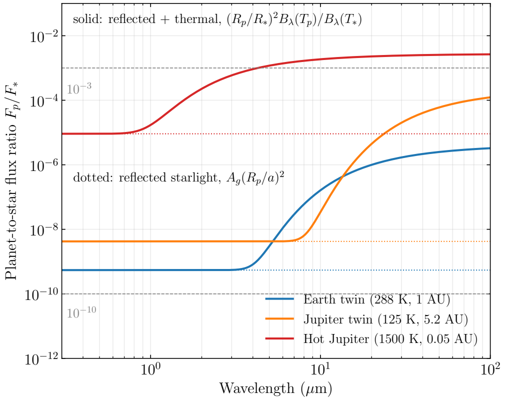

Figure 4: Planet-to-star flux ratio for three blackbody planets around a Sun-like star ($T_* = 5778$ K). Dotted lines: reflected light only, with a grey geometric albedo (0.3, 0.5, 0.1).

- In the **visible**, all three planets are 10^{-9}–10^{-5} fainter than the star: reflected light is set by $(R_p/a)^2$.
- In the **mid-infrared**, thermal emission takes over. An Earth twin reaches $\sim 10^{-7}$ at 10 µm; a Jupiter twin $\sim 10^{-4}$ only beyond ∼50 µm.
- A **hot Jupiter** — a Jupiter-sized giant planet orbiting its star at $a \sim 0.01$–0.1 AU (period of a few days), a hundred times closer than Jupiter, and heated by the intense starlight to $T_p \sim 1000$–2500 K — reaches the 10^{-3} level already at a few µm (curve for 1500 K, $a = 0.05$ AU): seven orders of magnitude easier than an Earth twin.

This is why the first atmospheric measurements were made in the infrared and for hot, close-in planets.

The Solar System planets: a reference table

Planet	a (AU)	P (yr)	$R_p/R_\oplus$	$M_p/M_\oplus$	ρ ($\mathrm{g\,cm^{-3}}$)	g ($\mathrm{m\,s^{-2}}$)	A_B	T_{eq} (K)	T_{surf}/T_{eff} (K)	main atmosphere
Mercury	0.387	0.24	0.383	0.055	5.43	3.7	0.12	434	100–700	none (Na, O exosphere)
Venus	0.723	0.62	0.949	0.815	5.24	8.9	0.75	230	735	92 bar: CO_2 96%, N_2 3.5%
Earth	1.000	1.00	1.000	1.000	5.51	9.8	0.31	253	288	1 bar: N_2 78%, O_2 21%
Mars	1.524	1.88	0.532	0.107	3.93	3.7	0.25	209	210	6 mbar: CO_2 95%, N_2 2.6%
Jupiter	5.20	11.9	10.97	317.8	1.33	24.8	0.34	109	124.4	H_2 90%, He 10%
Saturn	9.54	29.4	9.14	95.2	0.69	10.4	0.34	80	95.0	H_2 96%, He 3%
Uranus	19.19	84.0	3.98	14.5	1.27	8.9	0.30	58	59.1	H_2 83%, He 15%, CH_4 2%
Neptune	30.07	164.8	3.86	17.1	1.64	11.2	0.29	46	59.3	H_2 80%, He 19%, CH_4 1.5%

- T_{eq} is the **equilibrium temperature**, the temperature at which the planet reradiates exactly the stellar energy it absorbs, computed with uniform redistribution over the whole sphere. T_{surf} is the mean *surface* temperature of the terrestrial planets; T_{eff} is the measured **effective temperature** of the giants, i.e. the temperature of a blackbody radiating their total emitted flux.
- $R_\oplus = 6371\,\mathrm{km}$, $M_\oplus = 5.97\times10^{24}\,\mathrm{kg}$; $R_J = 11.2\,R_\oplus$, $M_J = 318\,M_\oplus$; 1 AU $= 1.496\times10^8$ km. Radii, masses, and compositions: NASA planetary fact sheets; albedos and temperatures: Seager (2010), Table 3.1 (after Cox 2000).

— The Solar System planets

- **Two families.** The densities split into $\rho \simeq 4$–$5.5\,\mathrm{g\,cm^{-3}}$ (rock and iron) and $\rho \simeq 0.7$–1.6 (H/He envelopes and ices), with nothing in between — and no planet at all between 1 and $3.9\,R_\oplus$. Filling that gap with super Earths and mini Neptunes was one of the surprises of the exoplanet surveys.
- **Gas giants versus ice giants.** Jupiter and Saturn hold 95–318 $M_\oplus$ of mostly hydrogen and helium; Uranus and Neptune are only 15–17 $M_\oplus$ and consist largely of water, methane, and ammonia ices, with a mere 1–2 $M_\oplus$ of H/He on top. That is why they are *denser* than Saturn despite being far less massive.
- **Super Earths and mini Neptunes** are the classes that fill the gap. A *super Earth* has 1–10 $M_\oplus$ (radius below ~ 1.5–$2\,R_\oplus$): predominantly rocky, with at most a thin outgassed atmosphere. A *mini Neptune* has 10–15 $M_\oplus$ (radius ~ 2–$4\,R_\oplus$): a rock and ice core wrapped in a few percent by mass of H/He, which is what inflates its radius. Both are common around other stars; we return to them under Types of Planets.

— The Solar System planets

- **Bond albedo A_B:** the fraction of the incident stellar *energy* — summed over all directions and all wavelengths — that the planet scatters back to space. The remaining fraction $(1 - A_B)$ is absorbed and eventually reradiated in the infrared. Venus is the brightest planet ($A_B = 0.75$, complete H_2SO_4 cloud cover) and Mercury the darkest (0.12, bare rock). Chapter 3 defines it precisely and distinguishes it from the geometric albedo A_g.
- Equating absorbed and reradiated energy gives the **equilibrium temperature**

$$T_{eq} = 279\,\mathrm{K}\,(1 - A_B)^{1/4}\left(\frac{a}{1\,\mathrm{AU}}\right)^{-1/2},$$

  so the orbital distance dominates and the albedo enters only through a fourth root: even Venus's very high albedo lowers T_{eq} by just 30%.
- **Two ways to depart from T_{eq}.** A *greenhouse* atmosphere raises the surface above it (Earth by 33 K, Venus by 505 K), while *interior heat* raises the emitted flux above the absorbed one, so that $T_{eff} > T_{eq}$ for Jupiter, Saturn, and Neptune — but not for Uranus, whose low heat flow is still unexplained.
- **Scale height $H = k_B T/mg$**, the altitude over which the pressure falls by e: 8.5 km (Earth), 15.9 (Venus), 11.1 (Mars), 27 (Jupiter), 60 (Saturn), 28 (Uranus), 20 (Neptune). It sets the size of a transmission signal (later this lecture).

From the Solar System to thousands of worlds

For centuries the debate was about *our* eight (or nine) planets: four rocky planets (Mercury, Venus, Earth, Mars) and four gas/ice giants (Jupiter, Saturn, Uranus, Neptune), flanked by the asteroid and Kuiper belts and the Oort cloud. This Solar-System-centric view was shattered in the 1990s:

- **1992** — planets around the pulsar PSR B1257+12 (Wolszczan & Frail), found from pulse-timing variations.
- **1995** — 51 Pegasi b (Mayor & Queloz), the first planet around a Sun-like star, from radial velocities: a **hot Jupiter**, a Jupiter-mass planet at $\sim$0.05 AU ($P = 4.2$ d) — a hundred times closer than Jupiter ($\sim$5 AU), heated to $\gtrsim 1000$ K.
- **2000** — HD 209458b, the first *transiting* planet (Charbonneau et al.; Henry et al.): radius, density, and soon after the first atmospheric detection.
- **2009** — *Kepler*: thousands of transiting planets; **super Earths** (radii between Earth and Neptune, absent from the Solar System) turn out to be *common*; compact multi-planet systems; circumbinary planets orbiting two stars.

Nature is far more creative at forming planets than our theories were. Each surprise forced a rethink of how the Solar System and other systems formed. Confirmed exoplanets now number in the thousands.

Milestones of exoplanet atmosphere observations

The hot Jupiter **HD 209458b** ($V \simeq 7.7$, $P = 3.5$ d, transit $\sim$3 h) became the benchmark: a bright host star means many photons per transit.

- **Brown et al. (2001):** HST/STIS transit light curve at a precision of $\sim$110 ppm per 80 s — proof that Earth-sized transit signals ($\sim$84 ppm) are within reach; a key step toward approval of *Kepler*.
- **Charbonneau et al. (2002):** first detection of an exoplanet atmosphere — excess transit depth of 232 ppm in the Na I doublet (589 nm), predicted by Seager & Sasselov (2000) because alkali metals stay gaseous at hot-Jupiter temperatures.
- **Vidal-Madjar et al. (2003):** 15% transit depth in Lyman-α — an extended, escaping hydrogen exosphere far beyond the Roche lobe (C and O detected in 2004).
- **Charbonneau et al. (2005); Deming et al. (2005):** first secondary eclipses with *Spitzer* — thermal emission from TrES-1 and HD 209458b.
- **Knutson et al. (2007):** first phase curve (HD 189733b at 8 μm) — a day–night map and evidence of winds.

Since then: HST/WFC3 water detections, ground-based high-resolution cross-correlation, and JWST spectra from $\sim$0.6 to 28 μm.

A theorist's view of the data

Planetary science studies the Solar System *in situ*. For exoplanets the answers to "What worlds exist? What is their chemical inventory? Which harbor life?" will come from *telescopes*.

Working knowledge of the data is therefore essential to build models that can be confronted with observations. The rest of this lecture reviews the observational techniques:

1. **Transits and occultations** — the "royal road": transmission spectra, emission spectra, albedos, phase curves, eclipse maps.
2. **Radial velocities** — masses, orbits, spin–orbit alignment, high-resolution atmospheric spectroscopy.
3. **Direct imaging** — spectra of young, self-luminous giants.
4. **Gravitational microlensing** — detection only.

Keep in mind throughout: *which physical quantity* is actually measured, and *what must be assumed* to turn it into a planetary property.

Path 1: direct imaging

The most natural idea: take a picture of the planet (as a point source), like photographing stars with a very good camera.

- Requires suppressing the starlight by 10^6–10^{10}: coronagraphs, adaptive optics (to cancel atmospheric blurring), or space telescopes.
- Currently limited to **big, bright, young or massive** substellar objects **far** from their stars (e.g. Fomalhaut b, Kalas et al. 2008; HR 8799 b,c,d, Marois et al. 2008). Young giants are still hot from formation, so the contrast can be as favorable as 10^{-4} in the near-IR.
- A solar-system-aged Earth or Jupiter twin is out of reach with current technology; space-based coronagraphs and starshades are being developed for this purpose (e.g. the Roman Space Telescope coronagraph, Habitable Worlds Observatory concept).

Fortunately, two *fortuitous, related* circumstances opened a completely different path.

Path 2: two fortunate circumstances

(1) A large population of planets orbits very close to their stars.

- Hot Jupiters, hot Neptunes, hot super Earths: orbital periods < 4 days, semimajor axes < 0.05 AU.
- Stellar heating brings hot Jupiters to 1000–2500 K, so their *infrared* brightness is $\sim 1/1000$ of the star's. Hard — but vastly better than the 10^{-10} visible contrast of an Earth twin.

(2) Many of these planets transit.

- The closer the planet, the higher the probability that its orbit is seen edge-on enough to cross the stellar disk ($P_{\text{transit}} \simeq R_*/a$; derived later).
- Short-period planets therefore guarantee a large sample of *transiting* planets.

The transit configuration lets us observe the atmosphere *without ever separating the planet's light from the star's*: everything is measured in the **combined light** of star + planet, as a function of time and wavelength.

Transit and secondary eclipse geometry

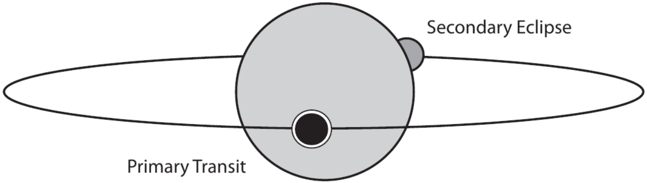

Figure 5: A transiting exoplanet passing in front of (primary transit) and behind (secondary eclipse) its star. The transparent annulus is the optically thin part of the atmosphere probed in transmission. Reproduced from Seager (2010), Fig. 1.3.

Primary transit. The starlight drops by the planet-to-star *area* ratio,

$$\delta = \frac{R_p^2}{R_*^2} \quad (\text{Jupiter/Sun: } 1\%,\ \text{Earth/Sun: } 8.4 \times 10^{-5}).$$

Given R_*, this yields R_p. Some starlight passes through the thin upper atmosphere and picks up its spectral features.

Secondary eclipse. Just before the planet goes behind the star, star + planet are seen together; during the eclipse only the star. The *difference* isolates the planet's dayside emission.

Both need only *differential* measurements in time — no spatial resolution.

The first thermal light curve: HD 189733b at 8 µm

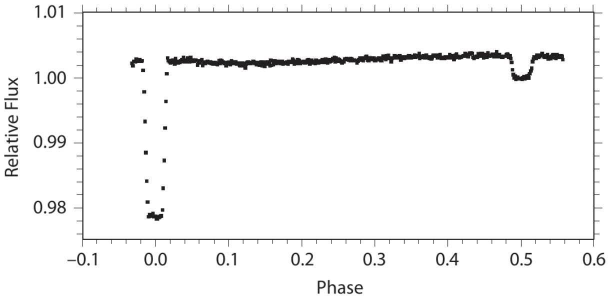

Figure 6: Spitzer 8 µm light curve of HD 189733 (star + planet). The first dip is the transit, the second the secondary eclipse. Data from Knutson et al. (2007); reproduced from Seager (2010), Fig. 1.4.

- HD 189733: a K dwarf with $R_* \simeq 0.75\,R_\odot$; the planet has $T \simeq 1200\,\mathrm{K}$ and $P = 2.2\,\mathrm{d}$.
- Transit depth $\simeq 2.4\%$ ($R_p/R_* \simeq 0.155$).
- Secondary-eclipse depth $\simeq 0.3\%$: at 8 µm this is the planet's *thermal emission*, so the depth gives the dayside **brightness temperature** (Chapter 3).
- Between the two dips the flux rises steadily: the **phase curve**, as more of the hot dayside rotates into view.

One light curve yields radius, dayside temperature, and a crude longitudinal temperature map.

Transit probability

How likely is it that a given planet transits? Half the angle subtended by the star as seen from the planet is

$$\tan\omega = \frac{R_*}{a} \quad \Longrightarrow \quad \omega \simeq \frac{R_*}{a} \quad (R_* \ll a).$$

An observer sees a transit only if the line of sight lies within $\pm\omega$ of the orbital plane: a **celestial band** of solid angle

$$\iint d\omega\, d\phi \simeq 2\pi \cdot 2\omega = \frac{4\pi R_*}{a}.$$

Dividing by the full sphere (4π sr),

$$\boxed{P_{\text{transit}} \simeq \frac{R_*}{a}} \quad \text{(circular orbit, random orientation).}$$

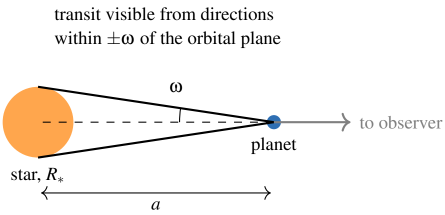

planet	a	P_{transit}
hot Jupiter	0.02–0.1 AU	5–50%
Earth	1 AU	0.5%
Jupiter	5.2 AU	0.09%

Consequences: hot Jupiters were found first; $P \propto R_*$ motivates searching for small planets around small (late-type M) stars, whose habitable zones are also close in.

Transit duration

If a planet transits, how long does it last? Consider a circular orbit crossing the stellar equator. The orbit has circumference $2\pi a$, and the chord across the star is $2R_*$, so the fraction of the orbit spent in transit is $R_*/(\pi a)$:

$$t_{\mathrm{transit}} = \frac{R_*\, t_{\mathrm{period}}}{\pi a}.$$

Kepler's third law (for $M_* \gg M_p$), $t_{\mathrm{period}} = 2\pi a^{3/2}/(GM_*)^{1/2}$, eliminates the period:

$$\boxed{t_{\mathrm{transit}} = 2R_* \left(\frac{a}{GM_*}\right)^{1/2} = \frac{2R_*}{v_{\mathrm{circ}}}} \qquad v_{\mathrm{circ}} = \sqrt{GM_*/a} \text{ the circular speed.}$$

- Hot Jupiter: 1–4 h; Earth: 13 h; Jupiter: 30 h.
- Weak scaling $t_{\mathrm{transit}} \propto a^{1/2}$: even a Jupiter at 100 AU transits for $\sim$130 h — but with $t_{\mathrm{period}} \sim 10^3$ yr and $P_{\mathrm{transit}} \sim 0.005\%$.
- Order-of-magnitude only. Eccentric or inclined orbits add correction factors of order unity (Winn 2010).
- In multi-planet systems, mutual gravitational perturbations make the orbits non-Keplerian: **transit timing variations (TTVs)** yield planet *masses* without radial velocities (Agol et al. 2005; Holman & Murray 2005).

Anatomy of a transit light curve

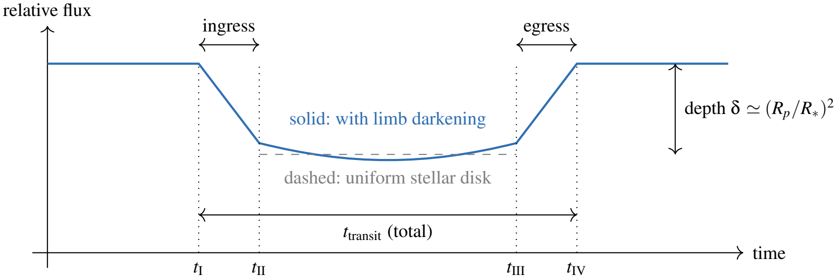

Four contact points bracket ingress ($t_{\text{I}} \to t_{\text{II}}$) and egress ($t_{\text{III}} \to t_{\text{IV}}$). The depth gives R_p/R_*; the total duration and the ingress/egress duration together give a/R_* and the impact parameter (orbital inclination) — the next two slides show how. Limb darkening rounds the bottom and blurs ingress/egress.

What the contact times encode: the transit chord

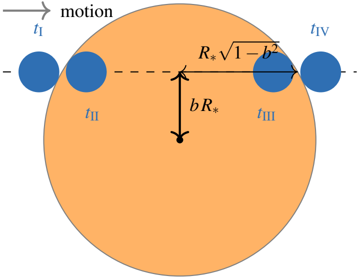

stellar disk, radius R_*

Because $a \gg R_*$, during the few hours of the transit the planet moves along an essentially *straight* chord across the stellar disk, at the constant sky-projected speed $v = 2\pi a/P$. Its projected separation from the star's center, in units of R_*, is

$$z(t) = \frac{a}{R_*}\sqrt{\sin^2\frac{2\pi t}{P} + \cos^2 i \cos^2\frac{2\pi t}{P}},$$

with t measured from mid-transit.

The chord's distance from the center of the disk at mid-transit defines the **impact parameter**

$$b \equiv z(0) = \frac{a\cos i}{R_*} \quad \text{(circular orbit)},$$

measured in stellar radii: $b = 0$ is a central transit, $b \to 1$ a grazing one, and $b > 1 + k$ means no transit at all ($k \equiv R_p/R_*$). It is a purely *geometric* quantity, equivalent to the inclination i.

The inclination i and the impact parameter b

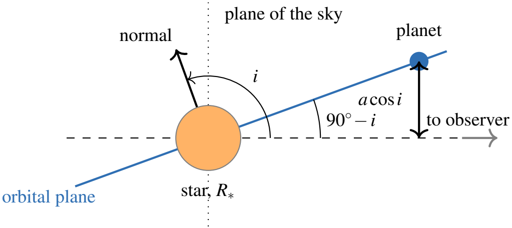

Side view, in the plane containing the line of sight and the orbit normal; the inclination is exaggerated.

Example: a hot Jupiter with $a/R_* = 10$ transiting at $b = 0.5$ has $\cos i = 0.05$, i.e. $i = 87.1^\circ$.

The **inclination** i is the angle between the orbital angular momentum — the normal to the orbital plane — and the line of sight: $i = 90^\circ$ is edge-on, $i = 0^\circ$ face-on.

- Seen from the side, the orbital plane therefore makes the angle $90^\circ - i$ with the line of sight.
- At mid-transit the planet lies a distance a from the star along that plane, so its offset *projected on the plane of the sky* is $a\sin(90^\circ - i) = a\cos i$.
- Dividing by the stellar radius gives the impact parameter,

$$\boxed{b = \frac{a\cos i}{R_*}}$$

which is why b and i carry the same information: the light curve measures b, and a/R_* converts it into i.

Transiting systems are nearly edge-on

A transit requires the two disks to overlap, $b < 1+k$, that is $\cos i < (R_* + R_p)/a$. Orbital orientations are random, i.e. uniform in $\cos i$, so the fraction of systems satisfying this is $(R_* + R_p)/a \simeq R_*/a$ — the transit probability derived earlier. The condition is very restrictive whenever the orbit is wide compared with the star:

system	a/R_*	$k = R_p/R_*$	transit requires
hot Jupiter ($a = 0.05$ AU, Sun-like star)	10.7	0.10	$i > 84.1°$
Earth–Sun	215	0.0092	$i > 89.73°$
Jupiter–Sun	1120	0.10	$i > 89.94°$

- Every transiting planet therefore has $\sin i \simeq 1$ to better than a fraction of a percent, so the radial-velocity quantity $M_p \sin i$ *is* the mass M_p: this is what makes the transit + RV combination yield a bulk density.
- A measured b still matters even so. Since $b = (a/R_*)\cos i$, one degree of inclination moves the chord by $\Delta b \simeq 0.19$ for a hot Jupiter, so the light curve constrains i far more tightly than the transit condition alone.
- The same geometry sets the secondary eclipse: on a circular orbit the planet passes behind the star half a period later with the same b, so a transiting planet almost always shows an occultation too.

The four contacts and the two durations

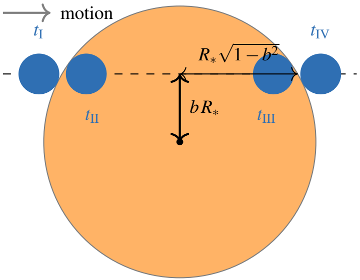

stellar disk, radius R_*

With $k \equiv R_p/R_*$, the contacts occur where the projected separation equals the sum or the difference of the two radii:

$$z = 1 + k \ \ (t_{\rm I}, t_{\rm IV}), \qquad z = 1 - k \ \ (t_{\rm II}, t_{\rm III}).$$

Half of the chord out to a contact at separation z has length $R_* \sqrt{z^2 - b^2}$, and it is traversed at the speed $v = 2\pi a/P$. Hence, for $a \gg R_*$ (so that $\sin i \simeq 1$ and the arc is a straight line),

$$T \simeq \frac{P}{\pi} \frac{R_*}{a} \sqrt{(1+k)^2 - b^2}, \qquad T_{\rm F} \simeq \frac{P}{\pi} \frac{R_*}{a} \sqrt{(1-k)^2 - b^2}.$$

- $T = t_{\rm IV} - t_{\rm I}$ is the **total duration**, $T_{\rm F} = t_{\rm III} - t_{\rm II}$ the **flat duration**, and $\tau = (T - T_{\rm F})/2$ the ingress (or egress) duration.
- Together with the depth $\delta = k^2$ and the period P, these are the observables from which k, b, and a/R_* follow.

Solving for k, b, and a/R_*

Three measured quantities (δ, T, T_F) plus the period determine the three unknowns (Seager & Mallén-Ornelas 2003):

- The **depth** gives the radius ratio, $k = \sqrt{\delta}$ (limb darkening corrections aside).
- The **ratio** of the two durations gives the impact parameter, because P and a/R_* cancel in $(T_F/T)^2 = [(1-k)^2 - b^2]/[(1+k)^2 - b^2]$:

$$\boxed{b^2 = \frac{(1-\sqrt{\delta})^2 - (T_F/T)^2\,(1+\sqrt{\delta})^2}{1-(T_F/T)^2}}$$

- The **absolute** duration then fixes the scaled semimajor axis:

$$\boxed{\frac{a}{R_*} = \frac{P}{\pi T}\sqrt{(1+\sqrt{\delta})^2 - b^2}}$$

  Up to the geometric factor, a/R_* is simply the ratio of the orbital period to the transit duration: a planet on a wide orbit spends a small fraction of its period in front of a small star.

- The inclination follows from $\cos i = b R_*/a$, and with the radial-velocity semi-amplitude it converts $M_p \sin i$ into M_p.

Why the *shape* measures b and the *duration* measures a/R_*

- **Central transit** ($b = 0$): the chord is a full diameter and $T_F/T = (1-k)/(1+k)$, close to 1 for small planets — a flat-bottomed, **U-shaped** light curve with a short ingress, $\tau/T \simeq k$.
- **Grazing transit** ($b \to 1-k$): the flat part disappears, $T_F \to 0$, and the ingress lasts half the event — a **V-shaped** light curve. In general, for $k \ll 1$,

$$\tau \simeq \frac{P}{\pi}\frac{R_*}{a}\frac{k}{\sqrt{1-b^2}} \qquad \Longrightarrow \qquad \frac{\tau}{T} \simeq \frac{k}{1-b^2}:$$

  the ingress lengthens as the chord shortens. The *shape* of the light curve carries b; the *absolute* duration then carries a/R_*.
- **Caveats.** Limb darkening blurs the contact points, so in practice one fits the entire light curve with a limb-darkened model (Mandel & Agol 2002) instead of reading off t_{I}–t_{IV}. For an eccentric orbit a is replaced by the instantaneous separation and the durations acquire the factor $\sqrt{1-e^2}/(1+e\sin\omega)$, so a/R_* becomes degenerate with e and ω. Near-grazing transits are also degenerate: b and k trade off against each other.
- **Why it matters.** a/R_* is model-independent geometry; combined with Kepler's third law it yields the stellar density (next slide), and it converts a measured eclipse depth into a geometric albedo, $A_g = D_{\mathrm{eclipse}}(a/R_p)^2$.

Stellar density from the light curve

Ingress and egress encode the **density of the star**. Writing the stellar mass as $M_* = \frac{4\pi}{3}\rho_* R_*^3$ and inserting it into Kepler's third law $GM_* = 4\pi^2 a^3 / t_{\rm period}^2$,

$$\boxed{\rho_* = \frac{3\pi}{G}\left(\frac{a}{R_*}\right)^3 t_{\rm period}^{-2}}$$

- $t_{\rm period}$: from repeated transits (very precise).
- a/R_*: directly from transit photometry, through the ingress/egress durations and the depth (Seager & Mallén-Ornelas 2003; Winn 2010).
- Hence a *model-independent* stellar density, a powerful anchor for stellar (and thus planetary) parameters.

Limb darkening. The optical depth τ decides whether a medium is transparent ($\tau \ll 1$) or opaque ($\tau \gg 1$). We see an "edge" to the Sun because we detect its $\tau \sim 1$ surface; since τ depends on wavelength, so does the stellar radius. Moreover, near the limb the line of sight reaches $\tau \sim 1$ in higher, cooler layers, so the projected disk has no sharp edge and is darker toward the limb. This smooths ingress/egress and rounds the bottom of the light curve (Mandel & Agol 2002). Extracting R_p correctly requires modeling limb darkening with stellar-atmosphere models.

Transmission spectra: the wavelength-dependent radius

To lowest order the transit radius is wavelength-independent. To next order it is not: the atmosphere absorbs starlight differently at different wavelengths. Let R_0 be the transit radius at a reference wavelength and $R = R_0 + \delta R$ at another. The change in transit depth is

$$\delta_{\rm transit} = \frac{\pi(R^2 - R_0^2)}{\pi R_*^2} \simeq \frac{2R_0\,\delta R}{R_*^2} \qquad \text{(annulus } 2\pi R_0 \delta R \text{ over stellar disk } \pi R_*^2\text{).}$$

δR is typically a few times the (isothermal) **pressure scale height**

$$\boxed{H = \frac{k_{\rm B}T}{mg}}$$

$k_{\rm B}$ Boltzmann constant, T temperature,
m mean molecular mass, g surface gravity.

The scale height is the altitude interval over which pressure falls by a factor e in hydrostatic equilibrium: $\mathrm{d}P/\mathrm{d}z = -\rho g$ with $P = \rho k_{\rm B} T/m$ gives $P \propto \mathrm{e}^{-z/H}$.

- Hot Jupiter ($T = 1000\,\mathrm{K}$, $g = 10^3\,\mathrm{cm\,s^{-2}}$, $m \simeq 2.3\,m_{\rm H}$): $H \simeq 400\,\mathrm{km} \Rightarrow \delta_{\rm transit} \sim 10^{-4}$.
- Earth-sized planet with the same H: $\delta_{\rm transit} \sim 10^{-5}$.
- Earth twin around a Sun-like star ($H \simeq 8\,\mathrm{km}$, N_2, $T = 290\,\mathrm{K}$): $\delta_{\rm transit} \sim 10^{-7}$ — a formidable feat.

The M-dwarf opportunity

Since $\delta_{\text{transit}} \propto R_*^{-2}$, a smaller star boosts *every* atmospheric signal:

host star	spectral type	$R_*/R_\odot$	boost $(R_\odot/R_*)^2$
Sun-like	G2	1.0	1
GJ 1214 (super Earth GJ 1214b)	M4.5	0.2	25
TRAPPIST-1 (seven Earth-sized planets)	M8	0.114	77

- A star with $R_* = 0.1\,R_\odot$ increases the transit depth of *any* atmosphere by a factor of 100.
- M dwarfs are also the most common stars, their habitable zones lie at $a \sim 0.02$–0.1 AU (high P_{transit}, frequent transits), and M_p/M_* is larger (bigger radial-velocity signal).
- Price: M dwarfs are faint, active (flares, spots), and their planets are tidally locked and strongly irradiated in the UV — questions of atmospheric retention.

There is a natural tension between planetary scientists, who want Earth-like planets around Sun-like stars, and astronomers, who need detectable signals; small stars are the pragmatic compromise.

How a transmission spectrum arises

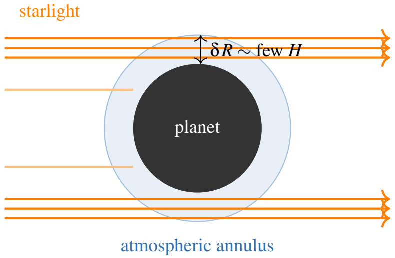

Starlight filters through the atmosphere along a long *chord* (slant path) at the day–night terminator. The chord — and thus the apparent radius — depends on wavelength.

Thought experiment: an atmosphere of pure water vapor.

- Where H_2O absorbs strongly, the atmosphere becomes opaque at high altitude → the planet looks *larger*.
- Where H_2O is transparent, starlight reaches deeper → the planet looks *smaller*.

Scanning the transit radius across wavelength gives the **transmission spectrum**, which encodes the atmospheric *opacity function* and identifies atoms and molecules.

The starlight travels *sideways* through the atmosphere rather than straight down, which makes the absorption far stronger than one might guess. In the ultraviolet, transmission probes the uppermost layers and constrains **atmospheric escape**.

Example: WASP-43b with HST/WFC3

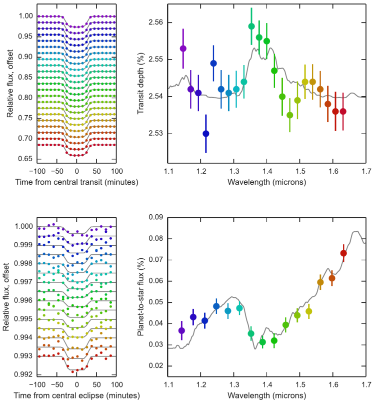

Figure 7: WASP-43b: transit light curves and transmission spectrum (top); eclipse light curves and emission spectrum (bottom). Kreidberg et al. (2014); Heng (2017), Fig. 1.1.

- Each colored light curve is one wavelength channel of the WFC3 grism (1.1–1.7 µm).
- **Transit depth** varies with wavelength by ∼0.03% (300 ppm): the bump peaking at 1.4 µm is the **water** band.
- The *widths* of the transit light curves change with wavelength because of stellar *limb darkening*; the *depths* change because of the atmosphere's opacity.
- **Eclipse depth** rises from 0.03% to 0.08% across the band: the dayside thermal emission spectrum, from which the temperature–pressure profile is retrieved. Note the precision required: tens of ppm per channel.

Secondary eclipse: emission spectra and geometric albedo

Occultation (secondary eclipse). The planet passes behind the star; the system shines only in starlight. Subtracting the in-eclipse flux from the flux just before eclipse isolates the *dayside* of the planet. The eclipse depth is

$$D_{\text{eclipse}} = \frac{F}{F + F_*} \simeq \frac{F}{F_*}$$

with F and F_* the wavelength-dependent fluxes of planet and star.

- Usually a smaller effect than the transit (10^{-3} in the IR, $\lesssim 10^{-4}$ in the visible for hot Jupiters).
- Extracting $F(\lambda)$ requires knowing $F_*(\lambda)$ and the star's peculiarities (activity, flares, starspots).
- **Infrared:** thermal emission dominates, $D \simeq (R_p/R_*)^2 B_\lambda(T_{\text{day}})/B_\lambda(T_{\text{eff}}) \Rightarrow$ dayside *brightness temperature*.

Geometric albedo. If the eclipse depth is measured where *reflected* starlight dominates (visible), then

$$A_g = D_{\text{eclipse}} \left(\frac{a}{R_p}\right)^2$$

is the albedo at zero phase angle. The **phase angle** α is the star–planet–observer angle: $\alpha = 0$ at secondary eclipse (dayside towards us), $\alpha = 180^\circ$ at transit. A Lambert sphere has $A_g = 2/3$, hot Jupiters are very dark ($A_g \lesssim 0.1$).

Phase curves: a one-dimensional map

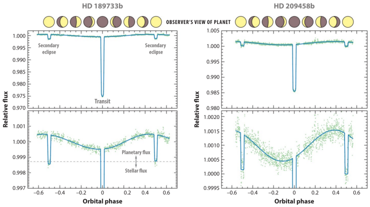

Figure 8: Infrared phase curves of HD 189733b (Knutson et al. 2007, 2009) and HD 209458b (Zellem et al. 2014). Heng (2017), Fig. 1.2.

Orbital phase φ: fraction of the period since transit (the horizontal axis). **Phase angle** α: star–planet–observer angle, with $\cos\alpha = -\cos 2\pi\varphi$ for a circular edge-on orbit.

	transit	eclipse
φ	0	0.5
α	180°	0°

As the planet orbits, it shows different faces to the observer; its brightness versus orbital phase is the **phase curve** (first measured for HD 189733b at 8 μm).

- The dips are transit (phase 0) and secondary eclipse (phase 0.5); the smooth modulation is the planet.
- Lower panels: the same data with the vertical scale expanded; the planetary flux is a few 10^{-3} of the stellar flux.
- It is a 1-D *longitudinal* (east–west) map of the brightness temperature, mixed with viewing geometry.
- Different wavelengths probe different pressures, giving limited 2-D (longitude–altitude) information.

Eclipse mapping: latitude too

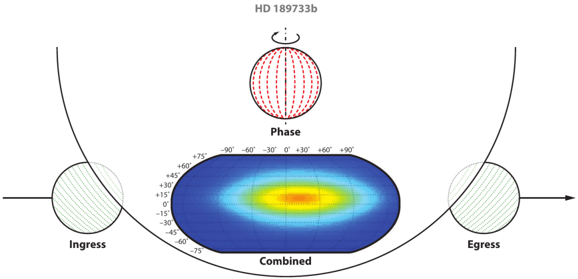

Figure 9: Eclipse mapping of HD 189733b (de Wit et al. 2012). Reproduced from Heng (2017), Fig. 1.3.

During ingress and egress of the *secondary eclipse*, the stellar limb scans across the planetary disk, hiding it strip by strip. High-cadence photometry of these moments recovers the brightness distribution along the direction of the scan.

- Phase curve → longitudinal information.
- Ingress/egress shapes → complementary (partly latitudinal) information.
- Combined → a 2-D map of the dayside.

Requires very high photometric precision *and* very precise orbital parameters (e.g. eccentricity): orbital uncertainties mimic the timing offsets produced by an asymmetric brightness distribution.

Putting it all together (1): transit and eclipse

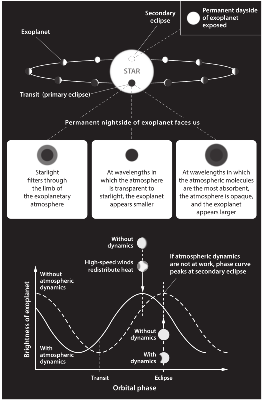

Figure 10: Phases of a transiting exoplanet, the resulting phase curve, and the influence of atmospheric dynamics. Heng (2017), Fig. 1.4.

The schematic unifies everything discussed so far. It assumes a **tidally locked** planet with permanent day and night sides, the normal situation for close-in planets (tidal synchronization times are $\ll$ the system age), but the principles apply generally.

- **Transit (primary eclipse):** the nightside faces us and starlight filters through the *limb* of the atmosphere. At wavelengths where the atmosphere is transparent the planet appears *smaller*; at wavelengths where its molecules absorb most strongly the atmosphere is opaque and the planet appears *larger*. This is the transmission spectrum.
- **Secondary eclipse:** the permanent dayside is fully exposed just before and after the planet passes behind the star; subtracting the in-eclipse flux gives the dayside emission spectrum and albedo.
- In between, the observer sees a changing mix of day and night hemispheres: the phase curve (next slide).

Putting it all together (2): phase curve and winds

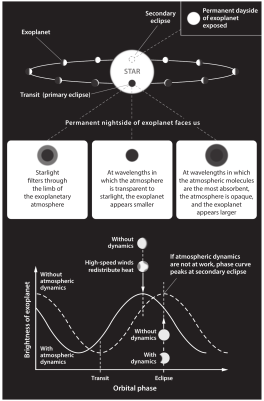

Figure 11: Same as the previous slide; the lower panel shows the phase curve with and without dynamics. Heng (2017), Fig. 1.4.

- **Without atmospheric dynamics:** the hottest point is the *substellar point* (the point on the planet at which the star is directly overhead, where the incident flux is greatest), and the brightness distribution is symmetric about it. The observer sees the maximum brightness when the full dayside is in view, so the phase curve *peaks exactly at secondary eclipse*.
- **With atmospheric dynamics:** high-speed winds (a super-rotating equatorial jet) advect heat away from the substellar point and shift the hot spot in longitude (eastward for hot Jupiters). Longitudes east of the substellar point face the observer *before* eclipse, so the brightness peak occurs *before* secondary eclipse.
- A measured **peak offset therefore implies winds** (Showman & Guillot 2002). For HD 189733b the 8 μm peak leads the eclipse by $\sim 16^\circ$ in longitude, and the day–night contrast is modest — efficient heat redistribution (Knutson et al. 2007).

Radial velocity measurements

The Sun and its planets orbit a common center of mass. As the star wobbles, its light is blue- and redshifted; the periodic Doppler shift is the **radial-velocity** (RV) signal — how 51 Peg b was found. The semi-amplitude of the stellar velocity is

$$K_* = \left(\frac{2\pi G}{t_{\mathrm{period}}}\right)^{1/3} \frac{M_p \sin i}{(M_* + M_p)^{2/3}} \left(1 - e^2\right)^{-1/2}$$

with i the orbital inclination and e the eccentricity.

- **The $M_p \sin i$ degeneracy:** RV alone gives a *minimum mass*. M_* comes from stellar-evolution models. If the planet *transits*, $\sin i \simeq 1$ and the true mass follows. Transit (R_p) + RV (M_p) $\Rightarrow$ bulk density and surface gravity $g = GM_p/R_p^2$ — essential input for interpreting any spectrum ($H = k_{\mathrm{B}}T/mg$).
- **Magnitudes:** hot Jupiter $K_* \sim 0.1\,\mathrm{km\,s^{-1}}$ (an order of magnitude faster than a sprinter); Jupiter (12-yr orbit) $\sim 10\,\mathrm{m\,s^{-1}}$; Earth $\sim 10\,\mathrm{cm\,s^{-1}}$ (humans walk at $\sim 1\,\mathrm{m\,s^{-1}}$). The technological demand grows steeply toward low masses.
- **Rossiter–McLaughlin effect:** a rotating star has a blueshifted approaching hemisphere and a redshifted receding one. A transiting planet blocks first one, then the other, producing an anomalous RV signal whose shape gives the sky-projected *spin–orbit misalignment*. Many hot Jupiters are misaligned — a clue to their migration history.

High-resolution spectroscopy of atmospheres

Ground-based spectrographs with resolution $\lambda/\Delta\lambda \sim 10^5$ (versus 10^2–10^3 for space-based low-resolution spectra) can also study atmospheres:

- The planet's own lines (in transmission or emission) shift by tens of $\mathrm{km\,s^{-1}}$ during the observation because of the planet's orbital motion, whereas stellar and **telluric** lines (from Earth's atmosphere) do not. This separates the three components.
- The thousands of individual molecular lines are too weak to see one by one; **cross-correlating** the residual spectrum with model templates of CO, H_2O, CH_4, … stacks them into a detectable signal (Snellen et al. 2010; Brogi et al. 2012).
- Yields unambiguous molecular identifications, the planet's orbital velocity (hence its true mass without $\sin i$), line Doppler shifts from winds, and even rotation.
- Extension: high-resolution *transmission* spectra of individual strong lines (Na, He 1083 nm, Hα) that probe the upper atmosphere and escape.

Low-resolution space spectroscopy and high-resolution ground-based spectroscopy are complementary: the former measures absolute band strengths, the latter line shapes and velocities.

Direct imaging

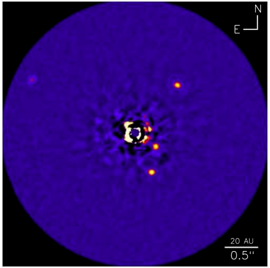

Figure 12: The four young gas-giant planets of HR 8799 (Marois et al. 2008, 2010), starlight suppressed. Heng (2017), Fig. 1.5.

Aim: directly photograph the planet and take its spectrum.

- The planet/star flux ratio is typically 10^{-6}–10^{-9} (infrared to visible) for mature planets. For **young** (10^7–10^8 yr) planets still flushed with their remnant heat of formation, the contrast can be as favorable as 10^{-4}.
- The starlight must be suppressed (coronagraph, adaptive optics, angular differential imaging) to isolate the planet and measure its emission spectrum $F(\lambda)$.
- HR 8799 b, c, d, e: 5–10 M_J planets at 15–70 AU; spectroscopy revealed H_2O and CO in their atmospheres (Barman et al. 2011; Konopacky et al. 2013).

Drawback: neither the radius nor the mass is measured directly; both are inferred from spectral and evolutionary models, which depend on the uncertain age and initial entropy, so they are *model-dependent*.
Strength: planets at wide separations, complementary to the close-in transiting population; and it is the path to Earth twins with future space coronagraphs and starshades.

Gravitational microlensing

Paczyński (1986) proposed that unseen objects in the Galactic halo act as gravitational lenses, which cause the transient brightening of a background star. He estimated the probability of such an event to be one in a million, implying that a million stars need to be monitored for it to be detected. Mao & Paczyński (1991) applied the same reasoning to the detection of planets.

- A foreground (lens) star passing in front of a background (source) star produces a smooth, symmetric rise and fall of the magnified light as the two move past each other. (Stars in our Galaxy are not static: they move at $\sim$10–100 km s^{-1}.)
- If a planet orbits the lens star, it distorts this smooth curve — a short-lived anomaly lasting hours to days, "in a manner analogous to astigmatism."
- The planet's mass ratio and projected separation (in units of the Einstein radius) follow from the shape of the anomaly.

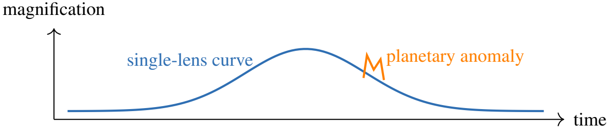

Microlensing: the Einstein radius and limitations

The characteristic length scale at which lensing occurs is the **Einstein radius**, the geometric mean of the Schwarzschild radius of the lens and the distance to the lens:

$$l_{\text{Einstein}} \sim \frac{(GM_* \, l_{\text{lens}})^{1/2}}{c}, \qquad l_{\text{Schwarzschild}} \sim \frac{GM_*}{c^2}$$

(order-of-magnitude form; the exact expression also involves the distance to the source and the lens–source separation).

- For a Sun-like lens at kpc distances, l_{Einstein} is a few AU. The numerical coincidence between this scale and the orbital distance of Jupiter-like planets ($a \simeq 5$ AU) makes the probability of detecting the planetary anomaly relatively high ($\sim 10\%$) once a stellar event is under way (Gould & Loeb 1992).
- **Limitations.** Microlensing detects planets (mass ratio, projected separation) but cannot characterize their atmospheres; the detection is *unrepeatable*; and the lens star is typically hard to distinguish photometrically from the source star, so the absolute planet mass needs extra information.
- **Strength.** Sensitivity to cold planets beyond the snow line, to low-mass planets, and to free-floating planets, at kpc distances toward the Galactic bulge — a demographic census that complements transits and radial velocities (the Roman Space Telescope microlensing survey).

Techniques compared

Technique	Measured quantities	Atmospheric potential	Main limitation / bias
Transit & eclipse	R_p/R_*, i, ρ_*, a/R_*; F/F_*, A_g, $T_{\rm day}$	High: transmission, emission, phase curves, eclipse maps	Needs edge-on geometry ($P \simeq R_*/a$); favors close-in planets
Radial velocity	$M_p \sin i$, e, $t_{\rm period}$; spin–orbit angle	Indirect: masses and g; high-resolution cross-correlation of molecular lines	Favors massive, close-in planets around quiet, slowly rotating stars
Direct imaging	Flux and emission spectrum $F(\lambda)$, astrometric orbit	Medium–high for young, hot giants; the route to Earth twins	Extreme contrast; wide separations only; M_p, R_p model-dependent
Microlensing	M_p/M_*, projected separation	None	Transient, unrepeatable; faint, distant hosts

Transit + RV is the most powerful combination: radius *and* mass give density, composition class, and surface gravity, which every atmospheric model needs.

The diversity of exoplanets

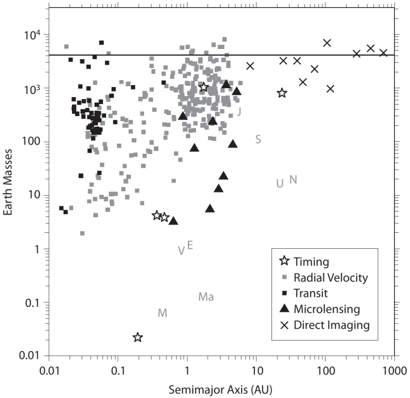

Figure 13: Known exoplanets as of January 2010, by discovery technique; circled points have an atmosphere measurement; Solar System planets by initial; the line is 13 M_J. Seager (2010), Fig. 1.5.

The most surprising aspect of exoplanets is their **broad diversity**: a nearly *continuous* range of masses and semimajor axes.

- Planet formation is *stochastic*: planets of many masses form at many locations in the protoplanetary disk.
- *Migration* carries planets very close to the star.
- The sloping lower envelope of the RV points is a *selection effect* ($K_* \propto M_p a^{-1/2}$); the mass of pulsar planets is known from timing.

We should expect a diversity of *atmospheres* rivaling the diversity of masses and orbits. Today (2026) the sample exceeds 6000 confirmed planets, dominated by *Kepler*/*TESS* transits, and the “desert” below the RV envelope has filled in.

The Solar System menagerie

Despite their different appearances, Solar System planets fall into two main categories.

Terrestrial planets — Mercury, Venus, Earth, Mars.

- Composed predominantly of rock and metals, with thin atmospheres.
- Atmospheres are *evolved*: escape of light gases and gas–surface reactions (weathering, ocean dissolution) have changed them substantially from their primitive state.
- Venus: 90 bar CO_2; Earth: 1 bar N_2/O_2; Mars: 6 mbar CO_2 — three very different outcomes.

Giant planets — Jupiter, Saturn, Uranus, Neptune.

- No rocky surface; masses up to hundreds of Earth masses.
- *Gas giants* (Jupiter, Saturn): almost entirely H and He, massive atmospheres, liquid metallic-hydrogen interiors.
- *Ice giants* (Uranus, Neptune): mostly water, methane, and ammonia "ices," with a 1–2 $M_\oplus$ H/He envelope.
- Atmospheres are *primitive*: little evolution, so they retain roughly the gases they formed with (solar-like H/He with enhanced heavy elements).

Gravity is the dividing line: heavy planets retain everything, including H_2 and He; light planets lose their light gases and keep only what is outgassed or supplied later.

Definitions (after Levine, Shaklan & Kasting 2006)

- **Planet:** an object that is gravitationally bound, supported against collapse by *electron degeneracy pressure* or *Coulomb pressure*, in orbit about a star, and that *never* sustains nuclear fusion in its core during its entire history. Theory puts this limit at $M_p \lesssim 13\,M_\mathrm{J}$ (deuterium burning). No convincing lower mass limit exists.
- **Exoplanet:** a planet orbiting a star other than the Sun (sometimes also used for free-floating planets without a host).
- **Terrestrial planet:** supported primarily by Coulomb pressure, with a *surface* defined by the radial extent of the solid interior or liquid outer layer ("rocky planet"); a thin gas atmosphere may exist above it.
- **Giant planet:** mass substantially above terrestrial but below brown dwarfs, $0.03\,M_\mathrm{J} < M_p < 13\,M_\mathrm{J}$ ($\sim 10\,M_\oplus < M_p \lesssim 4000\,M_\oplus$); interiors contain a substantial fraction of metallic hydrogen around a rocky core.
- **Brown dwarf:** 13–80$\,M_\mathrm{J}$; burns deuterium (and, above $\sim 65\,M_\mathrm{J}$, lithium) but never hydrogen. Their atmospheres are physically continuous with those of giant planets.

Habitability-related definitions

- **Habitable zone (HZ):** the region around a star in which a planet may maintain *liquid water on its surface*.
    - *Empirical* boundaries: Venus appears to have lost its water long ago (inner edge $\lesssim 0.75$ AU for the young Sun); Mars appears to have had surface water early on (outer edge $\gtrsim 1.5$ AU).
    - *Model* boundaries: runaway greenhouse (inner) and maximum CO_2 greenhouse (outer)[1], e.g. Kasting et al. (1993), Kopparapu et al. (2013).
- **Potentially habitable planet:** one whose orbit lies within the HZ.
- **Habitable planet:** a terrestrial planet on whose surface liquid water exists in steady state. This presumes that life, like Earth life, needs liquid water — and that the water and any life must be *at the surface* to be detectable remotely.
- **Earth-like planet:** similar to Earth in mass, radius, and temperature.
- **Earth twin:** an Earth-like planet with liquid-water oceans and continental land masses.

Being in the HZ is necessary but far from sufficient: Venus is near the HZ and the Moon is inside it. The atmosphere decides.

[1] **Runaway greenhouse:** more starlight evaporates more water, itself a strong greenhouse gas, so the surface warms and evaporates still more, until the ocean is in the atmosphere and its hydrogen escapes — Venus's likely history. **Maximum CO_2 greenhouse:** a cooling planet accumulates CO_2 to sustain warming; however, beyond a critical column depth, strong Rayleigh-scattering of incoming starlight causes net cooling and eventual atmospheric condensation, instead; the warming thus has a maximum, setting the outer edge.

Planets without Solar System counterparts

Class	Mass range	Composition	Atmosphere
Super Earth	1–10 $M_\oplus$	predominantly rocky (loosely defined)	thin, secondary (outgassed), or none
Mini Neptune	$\sim$10–15 $M_\oplus$	rock/ice core with gas envelope	H/He envelope, volatile-rich
Water world	—	$\geq 25\%$ water by mass	steam or H_2O-dominated; deep oceans
Carbon planet	—	more carbon than silicon (C/O $\gtrsim 1$ in the disk)	CO-, CH_4-, hydrocarbon-rich

These terms are loosely defined and partly overlap. Super Earths are intended to include predominantly rocky planets; mini Neptunes are planets of roughly 10–15 $M_\oplus$ with gas envelopes; water worlds and carbon planets are defined by bulk composition rather than by mass.

Super Earths, mini Neptunes, and the degeneracy problem

- Super Earths and mini Neptunes are the *most common* planets found by *Kepler*, yet they are absent from the Solar System. Their existence was one of the major surprises of the transit surveys.
- The boundary between them (rocky versus gas-enveloped) is now known to be a “radius valley” near 1.5–2 $R_\oplus$: planets below it have lost their primordial H/He envelopes, planets above it have retained a few percent by mass of H/He, which inflates the radius considerably (Fulton et al. 2017).
- Observations *cannot always distinguish* these planet types. A given mass and radius can be matched by different mixtures of iron, rock, water, and H/He — the well-known degeneracy of interior models. A $2\,R_\oplus$, $6\,M_\oplus$ planet may be a rocky core with a thin H/He envelope, or a water-rich world with a steam atmosphere.
- The *atmosphere* is often the crucial diagnostic: a hydrogen-dominated atmosphere has a large scale height and strong transmission features, whereas a heavy (H_2O, CO_2, N_2) secondary atmosphere has a small scale height and a nearly flat transmission spectrum. This is why the mean molecular mass m in $H = k_B T/mg$ matters so much.

Where do atmospheres come from?

There is no definitive classification of *atmosphere* types yet, but we expect a diversity as wide as that of orbits, masses, and radii.

Two origins.

- **Direct capture** of gas from the protoplanetary disk — for massive planets (Jupiter, Saturn): a *primary* atmosphere of H_2 and He with disk composition.
- **Outgassing** during and after accretion — for low-mass planets (Earth, Venus): a *secondary* atmosphere of H_2O, CO_2, N_2, … released from the solid material.

Sources versus sinks. The final mass and composition are the net result of

- *sources:* captured or outgassed gas — depending on the planet's *location* in the disk during formation, because of the disk's compositional gradients (snow lines of H_2O, CO_2, CO);
- *sinks:* atmospheric *escape* (thermal, hydrodynamic, non-thermal), *sequestration* of gases in oceans and crust (e.g. CO_2 into carbonates), and photochemical destruction.

The full range of atmospheric compositions remains to be uncovered, both theoretically and observationally. The formalism developed in this course is meant to be general enough to interpret *any* of them.

Future missions and telescopes

Predicting exact configurations is pointless, but the general investments are clear:

- **Space-based spectroscopy** from the UV to the infrared to build statistical samples of atmospheres and search for trends: HST (UV–near-IR) and **JWST** (0.6–28 μm, since 2022); **Ariel** (ESA, launch $\sim$2029) will survey $\sim$1000 transiting planets in transmission and emission.
- **Bright, nearby targets:** *CHEOPS* (2019), *TESS* (2018), and *PLATO* ($\sim$2026) greatly enlarge the sample of transiting planets around bright stars, the prerequisite for atmospheric follow-up.
- **Ground:** ever bigger mirrors (the 30–40 m class ELTs) with high-resolution spectrographs and extreme adaptive optics, to reach fainter sources and reflected light from nearby temperate planets.
- **Ultimately:** a space coronagraph or starshade (Habitable Worlds Observatory concept), or a fleet of formation-flying telescopes doing *interferometry*, to image an Earth twin and take its spectrum — the pale blue dot, again.

Take-home messages

Why atmospheres. Nearly everything we know about an exoplanet's temperature and composition comes from its atmosphere, observed as an unresolved point source through photometry and spectroscopy.

The obstacle. Not faintness but *contrast*: 10^{-10} for an Earth twin in the visible. Hot, close-in planets (10^{-3} in the infrared) and the *transit* configuration opened the field without direct imaging.

The royal road. Transit depth $\rightarrow R_p/R_*$; its wavelength dependence $\delta \simeq 2R_p \delta R/R_*^2$ with $\delta R \sim H = k_\mathrm{B} T/mg \rightarrow$ transmission spectrum; eclipse depth $F/F_* \rightarrow$ dayside emission, brightness temperature, albedo $A_g = D(a/R_p)^2$; phase curves and eclipse maps $\rightarrow$ winds. Probability R_*/a, duration $2R_*\sqrt{a/GM_*}$, stellar density from a/R_*.

Other tools. RV gives $M_p \sin i$ (mass when transiting), spin–orbit angles, and high-resolution molecular detections; direct imaging gives spectra of young giants; microlensing detects but does not characterize.

The zoo. Planets span a continuum of masses and orbits: terrestrial, giant, super Earth, mini Neptune, water and carbon worlds. Atmospheres are captured or outgassed, then shaped by escape and sequestration. Expect diversity.

References

- Seager, S. 2010, *Exoplanet Atmospheres: Physical Processes* (Princeton University Press), Chapter 1.
- Heng, K. 2017, *Exoplanetary Atmospheres: Theoretical Concepts and Foundations* (Princeton University Press), Chapter 1.
- Seager, S. and Deming, D. 2010, "Exoplanet Atmospheres," *ARA&A* **48**, 631.
- Sing, D. K. 2018, "Observational Techniques with Transiting Exoplanetary Atmospheres," in *Astrophysics of Exoplanetary Atmospheres* (Springer), Chapter 1.
- Winn, J. N. 2010, "Exoplanet Transits and Occultations," in *Exoplanets*, ed. S. Seager (Univ. Arizona Press), 55.
- Charbonneau, D., et al. 2000, *ApJ* **529**, L45; Charbonneau, D., et al. 2002, *ApJ* **568**, 377; Brown, T. M., et al. 2001, *ApJ* **552**, 699.
- Vidal-Madjar, A., et al. 2003, *Nature* **422**, 143.
- Knutson, H. A., et al. 2007, *Nature* **447**, 183; de Wit, J., et al. 2012, *A&A* **548**, A128; Kreidberg, L., et al. 2014, *ApJ* **793**, L27.
- Marois, C., et al. 2008, *Science* **322**, 1348; Kalas, P., et al. 2008, *Science* **322**, 1345.
- Snellen, I. A. G., et al. 2010, *Nature* **465**, 1049; Brogi, M., et al. 2012, *Nature* **486**, 502.
- Mao, S. and Paczyński, B. 1991, *ApJ* **374**, L37; Gould, A. and Loeb, A. 1992, *ApJ* **396**, 104.
- Levine, M., Shaklan, S., and Kasting, J. 2006, *Terrestrial Planet Finder STDT Report*, NASA/JPL D-34923.
- Turnbull, M. C., et al. 2006, *ApJ* **644**, 551; Pearl, J. C. and Christensen, P. R. 1997, *JGR* **102**, 10875.